Electronic Supplementary Material (ESI) for Journal of Materials Chemistry C.

Electronic Supplementary Information (ESI) for

4D printed shape memory metamaterial for vibration bandgap switching and active elastic-wave guiding

Bing Li, [a] Chao Zhang, [b] Fang Peng, [c] Wenzhi Wang, [a] Bryan D. Vogt [d, †] and K.T. Tan [b, *]

[a.] *School of Aeronautics, Northwestern Polytechnical University, Xi'an, Shaanxi, 710072, China*

[b.] *Department of Mechanical Engineering, The University of Akron, Akron, OH 44325-3903, USA*

[c.] *Department of Polymer Engineering, The University of Akron, Akron, OH 44325-3903, USA*

[d.] *Department of Chemical Engineering, The Pennsylvania State University, University Park, PA 16802, USA*

*Corresponding author E-mail address: [†] bdv5051@psu.edu, [*] ktan@uakron.edu

1. Meshing Size Effect

The local-resonance-induced bandgap frequencies related to Direction 1 and Direction 2 are numerically calculated under a series of meshing sizes and compared in Fig. S1. The normalized meshing size is defined as the ratio of meshing size to the unit cell thickness. As shown in Fig. S1, the two locally resonant frequencies decrease as the meshing goes from coarse to fine. At the smallest mesh sizes, the resonant frequencies approach to a converged value. To balance between the cost of computation time and the accuracy of the simulation, the normalized meshing size was set to 0.2 in this work.

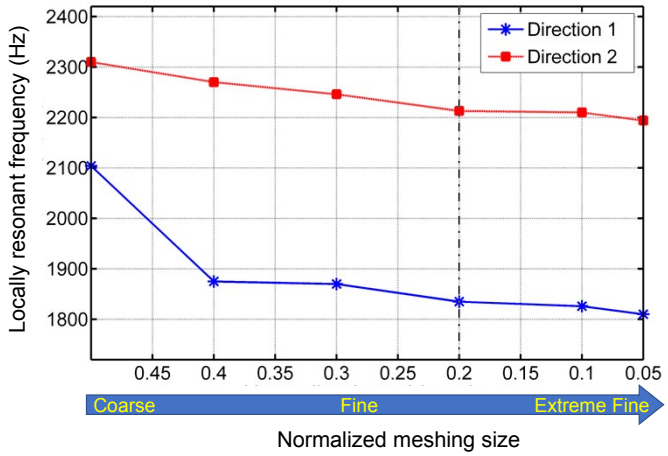

Fig. S1. Effect of meshing size on the calculated locally resonant frequencies.

2. Comparison of Dispersion Curve and Calculated Transmission Spectrum

A comparison of the measured dispersion curve and calculated transmission spectrum is shown in Fig. S2. As illustrated in Fig. S2(a), there are a series of full bandgaps along the ΓM direction for longitudinal and shear elastic-wave modes, as indicated by the yellow shading. Additionally, a series of flexural elastic-wave bandgaps are observed as indicated by the green shading. From Fig. S2, transmission attenuations are obvious around all bandgaps, providing good agreement between the experimentally measured dispersion curve and calculated transmission spectrum.

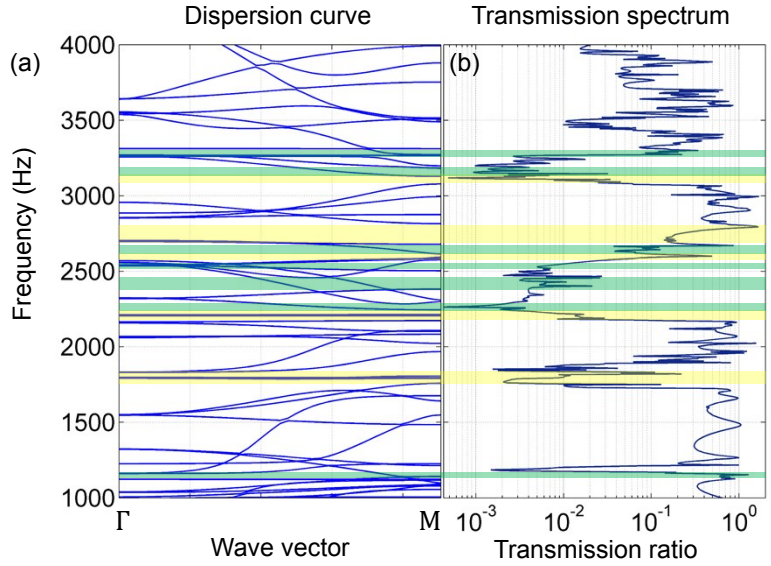

Fig. S2. Side by side comparison of the (a) dispersion curve and (b) transmission spectrum. Full bandgaps along the ΓM direction are shaded in yellow. Flexural elastic-wave bandgaps are shaded in green.

3. Evaluation of Manufacturing and Measurement Accuracy

For the 3D printed shape memory panel, the shape of three adjacent metamaterial unit cells, which are sequentially printed using identical 3D print manufacturing process, were selected to evaluate the manufacturing error. This was quantified using X-ray micro-computed tomography (μCT). Two dimensional reconstructions from μCT of the unit cells are shown in Fig. S3(a) and S3(b) for front and back views, respectively. Three pairs of "snow petals" inside the left, middle and right unit cells were extracted as shown in Fig. S4. The center lengths of all short and long

petals were quantified from the X-ray micro-computed tomography images (Table S1). The average length of long petals is 7.54 mm with a standard deviation of 0.09 mm, while the short petals are 4.63 mm with a standard deviation of 0.08 mm. These lengths agree well with the digital design. The errors in the dimensions from the manufacturing by 3D printing for the short and long petals range from -2.17% to 3.91% and -2.37 to 1.58%, respectively. From the measured petal lengths, the predicted bandgap frequencies were calculated based on Eq. (4) to understand the influence of the inaccuracy of the print on the designed bandgaps. The locally resonant frequency of the designed bandgaps can shift by less than 5% (-3.6% to 4.36%) from the observed imperfections in the manufacturing.

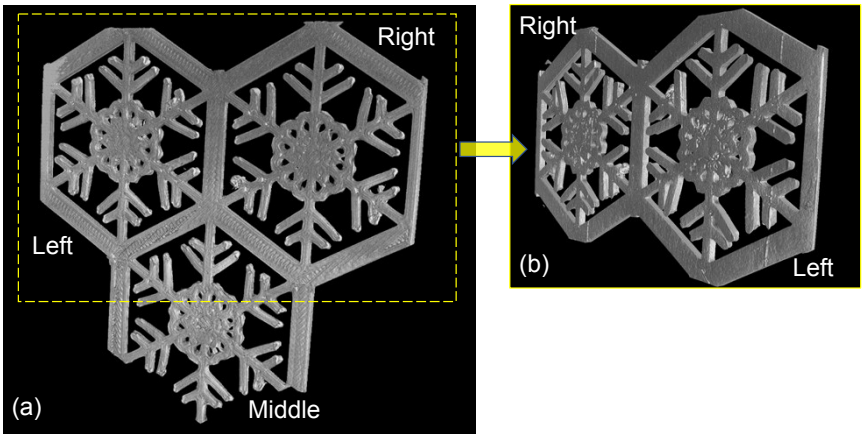

Fig. S3. Tomographic radiographs of the 3D printed unit cells for (a) front and (b) back views.

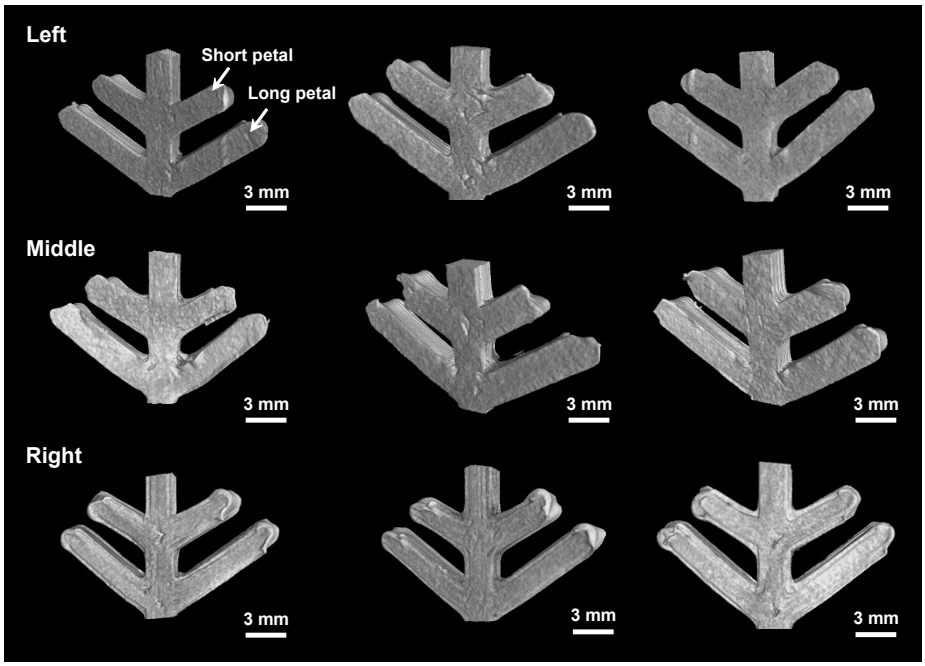

Fig. S4. Tomographic radiographs of the "snow petals" inside the left, middle and right unit

cells.

Table S1. Measured structural parameters of the 3D printed samples.

Unit cell	Length, long petal (mm)	Length, short petal (mm)
Left	7.52	4.67
	7.59	4.59
	7.46	4.64
	7.50	4.70
	7.48	4.50
	7.72	4.54
Middle	7.54	4.78
	7.46	4.69
	7.67	4.63
	7.42	4.66
	7.63	4.60
	7.60	4.69
Right	7.44	4.56
	7.48	4.54
	7.66	4.76
	7.48	4.53
	7.54	4.57
	7.55	4.64
Average	7.54	4.63
Standard deviation	0.087	0.080
Manufacturing relative error (%)	-2.37~1.58	-2.17~3.91
Predicted relative error (%) in bandgap	-3.60~4.36	

We supplement another round of test on the frequency response function to evaluate the measurement error. The tested transmission profile, which is obtained by 100 individual measurements and averaged automatically by the control system, is shown in Fig. S5 (see Test 2)) and compared with the previous test (Test 1). In general, the bandgap regions in the two tests agree well with each other, although slight mismatch occurs in the high frequency range. The frequencies of six typical bandgap dips (see f_1~f_6 in the transmission profiles) are selected for quantitative comparison. The relative errors between the two tests are listed in Table S2. It is observed that the maximum measurement relative error is around 5%, which is similar to the predicted error from the imperfections in the manufacture of the unit cell.

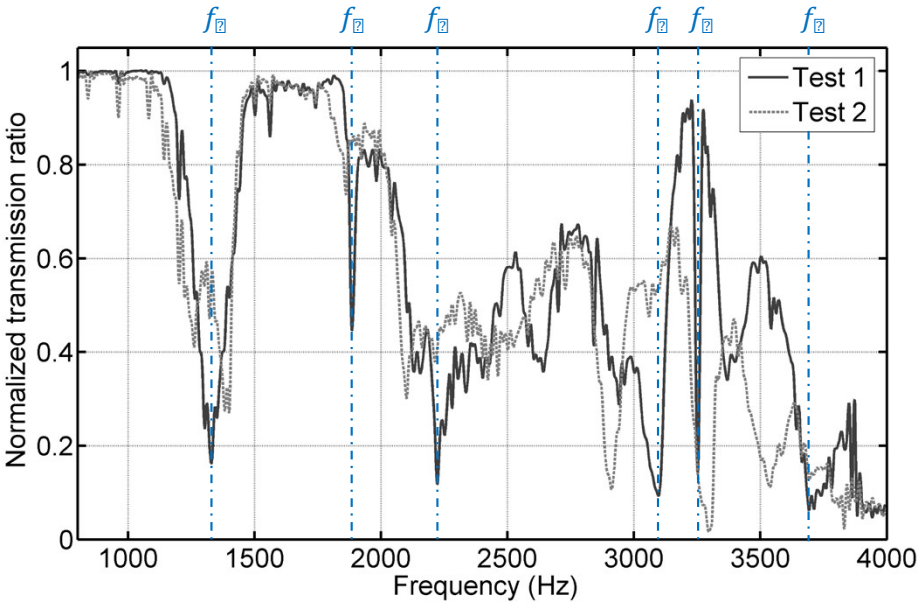

Fig. S5. Experimentally measured transmission-frequency profiles under two rounds of tests for the same structure.

Table S2. Measurement relative error of bandgap frequencies.

Bandgap dip frequency (Hz)	Test 1	Test 2	$\lvert Relative\ error \rvert$ (%)
f_1	1328	1401	5.50
f_2	1884	1863	1.11
f_3	2223	2101	5.49
f_4	3097	2914	5.91
f_5	3252	3295	1.32
f_6	3692	3541	4.09